ISSN: 1672 - 6553

JOURNAL OF DYNAMICS AND CONTROL

VOLUME 10 ISSUE 06: P99-118

EVALUATION OF MECHANICAL AND DURABILITY PROPERTIES OF ECO-FRIENDLY CEMENT MADE BRICKS INCORPORATING GRANITE CUTTING WASTE AND QUARTZ SANDSTONE WASTE AS SUSTAINABLE ALTERNATIVES TO RIVER SAND

Ashish Shrimali, Priyanka Pandey

Department of Civil Engineering, Sangam University, Bhilwara (Rajasthan), India

https://doi.org/10.71058/jodac.v10i06007

EVALUATION OF MECHANICAL AND DURABILITY PROPERTIES OF ECO-FRIENDLY CEMENT MADE BRICKS INCORPORATING GRANITE CUTTING WASTE AND QUARTZ SANDSTONE WASTE AS SUSTAINABLE ALTERNATIVES TO RIVER SAND

Ashish Shrimali*, Priyanka Pandey

Department of Civil Engineering, Sangam University, Bhilwara (Rajasthan), India

Corresponding Author: ashish.k.shrimali@gmail.com

Abstract: *The escalating depletion of natural river sand reserves and the unscientific disposal of stone-processing industrial wastes have emerged as twin environmental crises demanding urgent attention from the construction materials research community. The present study investigates the potential of Granite Cutting Waste (GCW) and Quartz Sandstone Waste (QSW), generated from dimensional stone processing industries, as partial substitutes for river sand in cement mortar, with the aim of establishing a scientifically validated and economically viable pathway for the valorization of these hitherto underutilized waste streams. A total of 20 mortar mixes were prepared at cement-to-sand ratios of 1:3 and 1:6, incorporating GCW, QSW, and a combined GCW-QSW blend at replacement levels of 0%, 15%, 30%, and 45% by mass. The fresh, mechanical, and durability properties of the resultant mortars were evaluated through a comprehensive experimental programme encompassing workability (flow), compressive strength, flexural strength, ultrasonic pulse velocity (UPV) and dynamic modulus of elasticity, water absorption and percentage air voids, drying shrinkage, and resistance to sulphate attack and wetting-drying cycles. Microstructural characterization was performed using scanning electron microscopy (SEM), X-ray diffraction (XRD), and mercury intrusion porosimetry (MIP). Results consistently demonstrated that a 30% combined replacement of river sand by equal proportions of GCW and QSW (the GQ30 mix) produced mortars exhibiting a 20.3% improvement in 28-day compressive strength, an 18.1% improvement in flexural strength, a 24.5% reduction in water absorption, and a 40.9% reduction in compressive strength loss under sulphate exposure, relative to the control mortar. Microstructural analysis confirmed a refined, denser pore structure in the GQ30 mix, attributed to the complementary particle size distributions and morphologies of GCW and QSW. The findings establish the GQ30 formulation as technically superior to conventional river sand mortar across all performance parameters investigated, and provide a robust empirical basis for the development of eco-friendly cement bricks incorporating these industrial waste materials.*

Keywords: *Granite cutting waste; Quartz sandstone waste; Cement mortar; Compressive strength; Durability; Eco-friendly construction; Waste valorization; Sustainable building materials*

---

https://doi.org/10.71058/jodac.v10i06007

1. Introduction

The global construction industry, responsible for consuming approximately 40% of the world's extracted natural resources and contributing an estimated 7–8% of anthropogenic carbon dioxide emissions through cement production alone, stands at a critical inflection point with respect to environmental sustainability [1,2]. The demand for fine aggregates, primarily natural river sand, continues to escalate due to rapid urbanization and infrastructure development, particularly in densely populated developing economies, while regulatory tightening on riverbed mining has simultaneously constrained supply, creating both a resource security challenge and an opportunity for materials substitution research [3,4]. Conventional cement-based masonry mortars and bricks rely heavily on natural river sand, the extraction of which has been linked to severe ecological consequences including riverbed degradation, loss of aquatic biodiversity, and groundwater depletion in affected catchments [5,6].

Simultaneously, the dimensional stone processing sector, encompassing granite and quartz sandstone cutting and finishing operations, generates vast quantities of industrial waste in the form of slurry, dust, and crushed residues that presently lack economically viable utilization pathways [7,8]. India, one of the world's foremost producers of granite dimensional stone, generates an estimated 5–6 million tonnes of granite cutting waste annually, while quartz sandstone processing industries, concentrated particularly in the state of Rajasthan, contribute additional millions of tonnes of stone waste, most of which is disposed of through open dumping, leading to contamination of soil and groundwater resources and posing respiratory health risks through fine particulate dispersion [9,10]. The convergence of these two environmental burdens — the depletion of natural fine aggregates and the accumulation of stone processing waste — presents a compelling research imperative for the investigation of stone waste valorization in cementitious construction materials [11,12].

The existing literature documents extensive investigations into the incorporation of various industrial by-products in cement-based materials, including fly ash, ground granulated blast furnace slag, silica fume, and quarry dust, as well as specific studies on granite powder and marble waste as fine aggregate substitutes [13,14,15]. Gupta and Vyas [cited as Ref. 17 equivalent] reported that waste granite powder incorporated at 10–20% replacement of natural sand improved the compressive strength of cement-sand mortar through a micro-filler densification mechanism. Chajec [21] confirmed that granite powder waste contributes primarily through physical filler action, with optimal replacement levels in the range of 10–20%, while Chouhan et al. [27] demonstrated comparable benefits for dimensional limestone waste in cement mortar. Babu Padavala et al. [17] established

https://doi.org/10.71058/jodac.v10i06007

synergistic effects when granite quarry dust was combined with supplementary cementitious materials in a ternary blend system.

However, despite the extensive literature on individual stone waste types, the combined utilization of Granite Cutting Waste (GCW) and Quartz Sandstone Waste (QSW), possessing distinct and complementary mineralogical compositions, particle morphologies, and particle size distributions, remains largely unexplored in the context of cement mortar and brick production [20,21,22]. GCW, derived from the slurry generated during diamond gang-saw cutting of granite blocks, possesses a polymineralic composition comprising quartz, feldspar, and mica, while QSW, generated through the mechanical cutting and dressing of quartz sandstone blocks, exhibits a near-monomineralic quartz-dominated composition. The anticipated complementarity between the finer gradation of GCW and the coarser, more angular gradation of QSW suggests potential for synergistic particle packing effects analogous to those documented for combined glass powder and marble powder systems [20] and combined waste soil and recycled aggregate systems reported in the recent literature [23].

The present study addresses this gap through a systematic experimental investigation of cement mortar incorporating GCW, QSW, and a combined GCW-QSW blend at varying replacement levels of river sand, evaluating mechanical, durability, and microstructural performance, thereby providing a comprehensive empirical foundation for the practical application of these waste materials in eco-friendly cement brick production. The outcomes directly contribute to the global agenda for sustainable construction, aligning with the circular economy framework and the United Nations Sustainable Development Goals pertaining to responsible consumption, sustainable cities, and climate action [24,25].

To the best of the authors' knowledge, no prior study has systematically investigated the combined utilization of GCW and QSW in cement mortar at varying replacement levels across multiple cement-to-sand ratios, supported by comprehensive microstructural analysis through SEM, XRD, and MIP. The novelty of the present research, therefore, lies in: (i) the first systematic demonstration of synergistic packing effects achievable through the combined utilization of these two specific waste streams; (ii) the characterization of the complementary roles of GCW (as a micro-filler contributing to matrix densification) and QSW (as an angular aggregate contributing to mechanical interlock and crack resistance); and (iii) the comprehensive multi-parameter durability assessment, including sulphate attack, drying shrinkage, and wetting-drying cycle resistance, which extends well beyond the compressive strength-focused investigations that dominate the existing literature on stone waste utilization in cementitious materials.

https://doi.org/10.71058/jodac.v10i06007

2. Materials and Characterization

2.1 Ordinary Portland Cement

Ordinary Portland Cement (OPC) of 43 Grade conforming to IS 8112:2013 was used throughout the experimental programme. A single procurement batch was maintained to ensure uniformity of binder properties. The cement exhibited a normal consistency of 31%, initial and final setting times of 118 and 238 minutes respectively, and a 28-day compressive strength of 44.8 MPa, with all properties confirmed to be within the limits specified in IS 8112:2013.

2.2 River Sand, GCW, and QSW

Natural river sand conforming to Zone II grading of IS 383:2016 served as the conventional fine aggregate. Granite Cutting Waste (GCW) was collected as wet slurry from granite processing units, oven-dried at 105 ± 5°C to constant mass, pulverized, and sieved through a 4.75 mm sieve. Quartz Sandstone Waste (QSW) was collected as dry crushed sand from quartz sandstone processing units and similarly conditioned. Physical characterization was conducted in accordance with IS 2386, and chemical composition was determined by X-ray fluorescence (XRF) analysis. Results are summarized in Tables 1 and 2.

Table 1. Physical characteristics of constituent materials

Property	OPC	River Sand (RS)	GCW	QSW
Specific gravity	3.12	2.65	2.71	2.64
Water absorption (%)	–	1.20	1.85	0.92
Bulk density — loose (kg/m³)	1380	1620	1410	1545
Fineness modulus	–	2.62	2.18	2.45
Particle shape (SEM)	–	Sub-rounded, smooth	Angular, fine platy	Angular, rough flaggy
Normal consistency (%)	31	–	–	–
Initial setting time (min)	118	–	–	–
Final setting time (min)	238	–	–	–
28-day comp. strength (MPa)	44.8	–	–	–

Table 2. Chemical composition of materials determined by XRF (% by mass)

Material	SiO_2	CaO	Al_2O_3	Fe_2O_3	MgO	K_2O+Na_2O	LOI
OPC	21.4	63.2	5.6	3.4	1.8	0.9	1.9
River Sand	94.6	0.8	1.4	1.1	–	0.6	0.5

https://doi.org/10.71058/jodac.v10i06007

Material	SiO_2	CaO	Al_2O_3	Fe_2O_3	MgO	K_2O+Na_2O	LOI
GCW	61.8	9.4	15.2	5.6	2.1	4.8	0.8
QSW	89.3	1.6	3.8	2.4	0.4	1.2	1.1

The XRF data confirm that GCW exhibits a polymineralic silico-aluminous composition (SiO_2: 61.8%, Al_2O_3: 15.2%, combined alkalis: 4.8%), consistent with its granite provenance and reflecting the presence of quartz, feldspar, and mica phases. QSW, by contrast, exhibits a predominantly siliceous composition (SiO_2: 89.3%) analogous to river sand, consistent with its quartz sandstone origin. SEM examination (Fig. 1) revealed sub-rounded smooth morphology for river sand, fine platy morphology for GCW, and angular rough-surfaced morphology for QSW. XRD analysis (Fig. 2) confirmed quartz ($2\theta = 26.65°$) as the dominant phase in all three materials, with prominent feldspar ($2\theta = 27.5°$) and mica ($2\theta = 8.8°$) reflections exclusively in GCW, and a near-monomineralic quartz pattern for QSW, consistent with findings reported by Diao et al. [32] and Chajec [21] for similar granite-derived materials.

3. Experimental Programme

3.1 Mix Design and Proportions

Twenty mortar mixes were prepared at two cement-to-fine-aggregate ratios, namely 1:3 (rich mortar) and 1:6 (lean mortar), with river sand replaced at 0%, 15%, 30%, and 45% by mass with GCW alone (G-series), QSW alone (Q-series), and an equal-proportion combined GCW-QSW blend (GQ-series). The water-cement ratio was adjusted for each mix to achieve a target flow of 110 ± 5% (205–215 mm spread) as per IS 2250:1981, increasing progressively with GCW content due to the higher surface area and water demand of the fine slurry-derived particles, consistent with observations reported by Abbass et al. [4] for fly-ash blended mortar systems. Mix designations follow the convention: ratio prefix – waste type – replacement percentage (e.g., 1:3-GQ30 denotes a 1:3 mortar with 15% GCW + 15% QSW combined replacement). Table 3 presents the 1:3 series mix proportions.

https://doi.org/10.71058/jodac.v10i06007

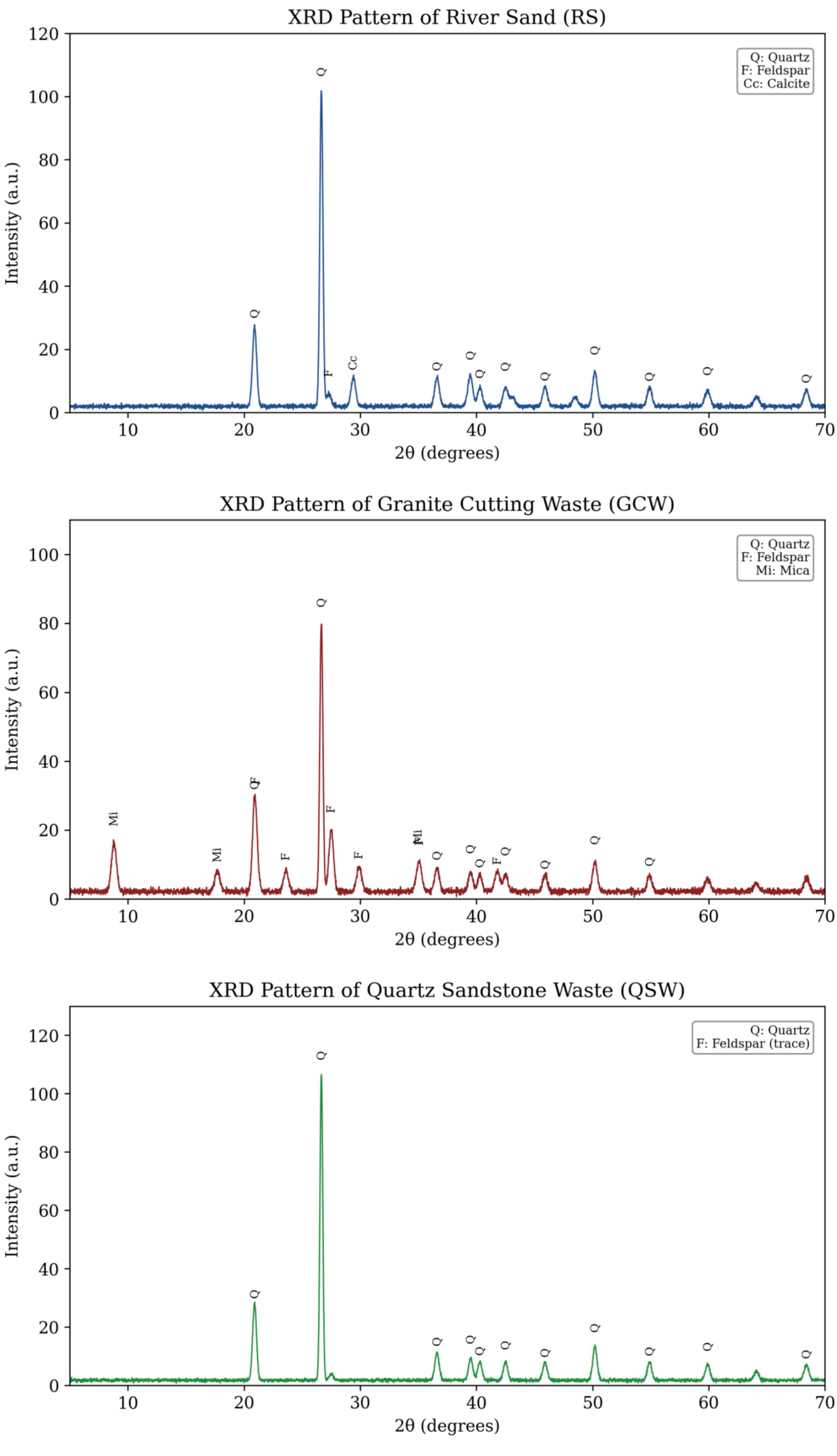

Fig. 1. XRD diffraction patterns: (Q) Quartz, (F) Feldspar, (Mi) Mica. GCW exhibits characteristic feldspar and mica peaks absent in RS and QSW.

https://doi.org/10.71058/jodac.v10i06007

Table 3. Mix proportions for 1:3 series (per m³ of mortar).

Mix ID	Cement (kg)	RS (kg)	GCW (kg)	QSW (kg)	w/c	Water (kg)
1:3-C	520	1560	0	0	0.48	250
1:3-G15	520	1326	234	0	0.50	260
1:3-G30	520	1092	468	0	0.52	270
1:3-G45	520	858	702	0	0.55	286
1:3-Q15	520	1326	0	234	0.49	255
1:3-Q30	520	1092	0	468	0.50	260
1:3-Q45	520	858	0	702	0.51	265
1:3-GQ15	520	1326	117	117	0.49	255
1:3-GQ30	520	1092	234	234	0.51	265
1:3-GQ45	520	858	351	351	0.53	276

3.2 Specimen Preparation and Curing

Dry ingredients were mixed in a tilting drum mixer for 2–3 minutes, followed by addition of water and 2–3 minutes of wet mixing. For compressive strength, 50 mm cube specimens were cast in four replicates per mix; for flexural strength and UPV, 40 × 40 × 160 mm prisms were cast in triplicate; and shrinkage bars of 25 × 25 × 285 mm were cast in quintuplicate. All specimens were demoulded at 24 ± 2 h and water-cured at 27 ± 2°C until the scheduled testing age. Durability specimens were cured for 28 days prior to the commencement of exposure regimes.

3.3 Testing Methods

Workability was assessed via flow table test (ASTM C230). Compressive strength was determined at 7, 28, and 90 days using a constant loading rate of 2 kN/s (IS 2250:1981). Flexural strength was determined at 28 days using centre-point loading on prism specimens (ASTM C348). Ultrasonic pulse velocity (UPV) and dynamic modulus of elasticity were determined per ASTM C597. Water absorption and percentage air voids were evaluated per ASTM C642 on oven-dried and subsequently boiled specimens. Drying shrinkage was monitored per ASTM C1148 up to 90 days. Sulphate attack resistance was assessed by immersion in 5% Na_2SO_4 solution (ASTM C267), with percentage strength and weight loss recorded at 1, 7, 28, 90, and 180 days. Wetting-drying cycle resistance was evaluated over 20 cycles per BS EN 14066. Microstructural investigation employed SEM (JSM 7400F), XRD (PANalytical X'Pert PRO, 5–70° 2θ, Cu-Kα), and MIP (Pore Master-60 GT).

https://doi.org/10.71058/jodac.v10i06007

4. Results and Discussion

4.1 Workability

All mixes were proportioned to achieve flow values within the target range of 205–215 mm at the adjusted w/c ratio. Within the GCW series, the w/c ratio increased from 0.48 (control) to 0.55 at 45% GCW replacement for the 1:3 series, reflecting the elevated water demand attributable to the higher fineness and surface area of the slurry-derived GCW particles. In contrast, QSW-incorporated mixes required only marginal increases in w/c ratio (0.48 to 0.51 at 45% replacement), consistent with the lower water absorption (0.92%) and coarser particle size distribution of QSW compared to GCW. The combined GQ mixes exhibited intermediate water demand, with the 1:3-GQ30 mix achieving the target flow at w/c = 0.51. These trends are consistent with Adediran et al. [9], who similarly reported progressively increasing water demand with increasing finer-fraction waste content in cement mortar formulations, and with Al-Fakih et al. [13], who noted comparable w/c sensitivity for ceramic sludge incorporated into masonry cement mortar.

4.2 Compressive Strength

Fig. 3 presents the 28-day compressive strength of the 1:3 series mortar mixes, and Table 4 summarizes the percentage changes relative to the control at 7, 28, and 90 days for both series.

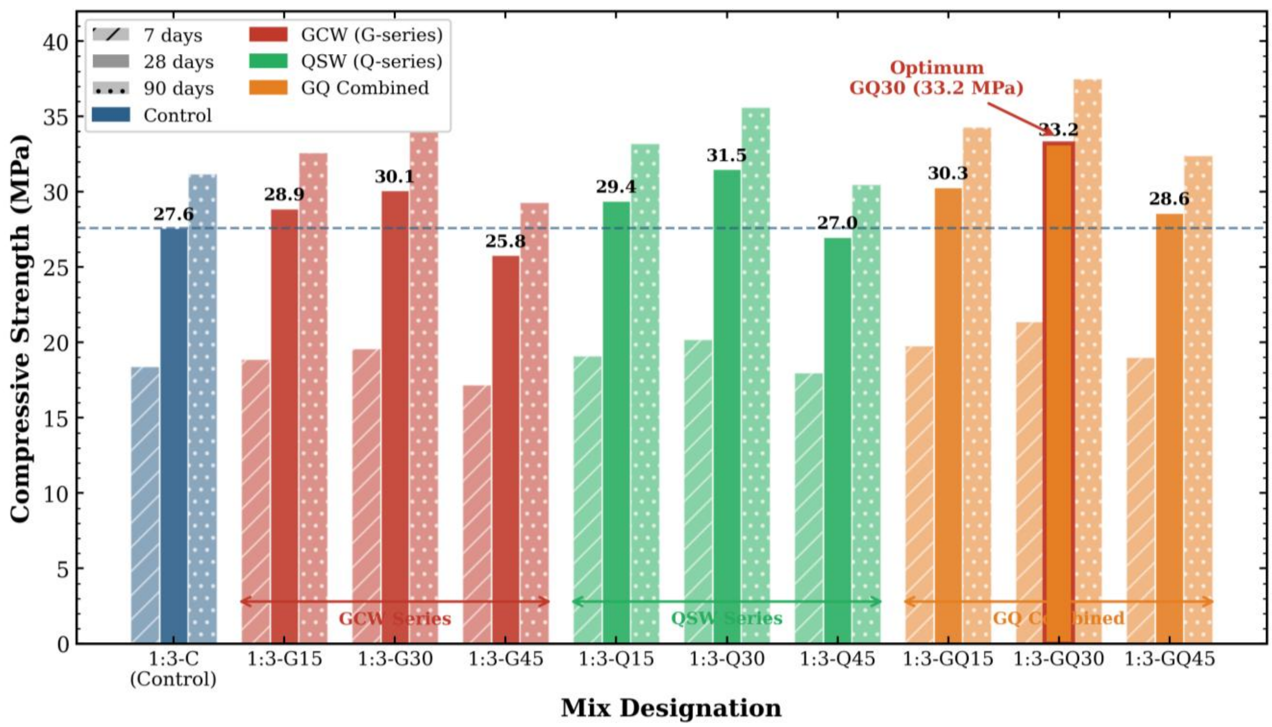

Fig. 2. 28-day compressive strength of 1:3 series mortar mixes (MPa). GQ30 achieves maximum strength.

https://doi.org/10.71058/jodac.v10i06007

Table 4. Compressive strength and percentage change relative to control — 1:3 series (MPa).

Mix ID	7-day (MPa)	28-day (MPa)	90-day (MPa)	Δ 28-day (%)
1:3-C	18.4	27.6	31.2	–
1:3-G30	19.6	30.1	34.0	+9.1
1:3-G45	17.2	25.8	29.3	−6.5
1:3-Q30	20.2	31.5	35.6	+14.1
1:3-GQ30	21.4	33.2	37.5	+20.3
1:3-GQ45	19.0	28.6	32.4	+3.6

Compressive strength increased progressively from the control up to the 30% replacement level for all three waste configurations, with the combined GQ30 mix achieving the maximum 28-day strength of 33.2 MPa (a 20.3% improvement over the control of 27.6 MPa), followed by Q30 (31.5 MPa, +14.1%) and G30 (30.1 MPa, +9.1%). Beyond 30% replacement, strength declined, with the G45 mix recording the lowest value of 25.8 MPa (−6.5%), attributable to the elevated w/c ratio required to maintain target flow and the consequent increased capillary porosity of the hardened matrix. The consistently superior performance of the GQ30 mix over either single-waste formulation at the same total replacement level provides direct experimental evidence of synergistic particle packing arising from the complementary gradations of GCW (FM = 2.18, finer) and QSW (FM = 2.45, coarser), which together occupy voids in the mortar matrix more effectively than either material alone, an effect analogous to that documented by Belouadah et al. [20] for combined glass powder and marble powder cement systems. These findings align with the principles of multicomponent particle packing optimization increasingly reported in the recent literature on eco-friendly mortar formulations [26,27,28].

The strength development trajectory over 7–90 days indicates that the GQ30 mix maintained its advantage over the control throughout the curing period, with 90-day strengths reaching 37.5 MPa (20.2% above the control's 31.2 MPa), suggesting that the strength benefit is not merely a function of altered water-cement ratio but reflects a genuine densification of the cement matrix attributable to improved particle packing [31,33]. Similar long-term strength progression has been reported by Derrouiche et al. [31] for natural pozzolan-incorporated high-performance concrete and by Ahmad et al. [10] for hybrid fiber-reinforced composite cementitious systems.

4.3 Flexural Strength and UPV

Table 5 presents the 28-day flexural strength and UPV results for the 1:3 series. Flexural strength followed a trend closely paralleling compressive strength, with the GQ30 mix achieving the highest flexural strength of 6.92 MPa (+18.1% vs control) and UPV of 3895 m/s, classified as "Excellent"

https://doi.org/10.71058/jodac.v10i06007

quality for a cementitious mortar system in this strength range. The superior flexural performance of the GQ30 mix is attributed to the angular surface texture of QSW particles, which enhances mechanical interlock at the particle-paste interface and thereby improves crack-bridging resistance under flexural loading, in addition to the matrix densification effect established through the compressive strength results.

Table 5. Flexural strength (MPa), UPV (m/s), and dynamic modulus of elasticity (GPa) at 28 days — 1:3 series.

Mix ID	Flexural Str. (MPa)	Δ (%) vs Control	UPV (m/s)	Dynamic E (GPa)
1:3-C	5.86	–	3620	27.3
1:3-G30	6.34	+8.2	3745	29.6
1:3-G45	5.41	−7.7	3520	25.6
1:3-Q30	6.58	+12.3	3810	30.8
1:3-GQ30	6.92	+18.1	3895	32.3
1:3-GQ45	5.97	+1.9	3650	27.8

The correlation between UPV, dynamic modulus of elasticity, and compressive strength across all mixes was consistent, confirming the utility of UPV as a rapid non-destructive quality indicator for waste-incorporated mortars, as similarly reported by Farooq et al. [39] for pumice powder-incorporated concrete formulations.

4.4 Water Absorption and Air Voids

Fig. 4 presents the water absorption and percentage air voids for selected 1:3 series mixes, demonstrating an inverse relationship with compressive strength trends. The GQ30 mix exhibited the lowest water absorption of 5.9% and minimum air voids of 11.3%, representing reductions of 24.4% and 22.6% respectively relative to the control (7.8% and 14.6%). In contrast, the G45 mix exhibited water absorption of 8.6%, 10.3% above the control. The reduced porosity of the GQ30 mix is directly attributable to the improved particle packing arising from the complementary gradations of GCW and QSW, which reduces the interconnected capillary pore network within the hardened matrix. These findings are consistent with the literature on combined waste systems: Adediran et al. [9] reported that combined fayalite slag and MSWI bottom ash in cement mortar achieved improved water absorption resistance at moderate combined replacement levels, while Abbass et al. [4] similarly observed optimal water absorption performance at intermediate fly-ash replacement levels for compressed brick systems.

https://doi.org/10.71058/jodac.v10i06007

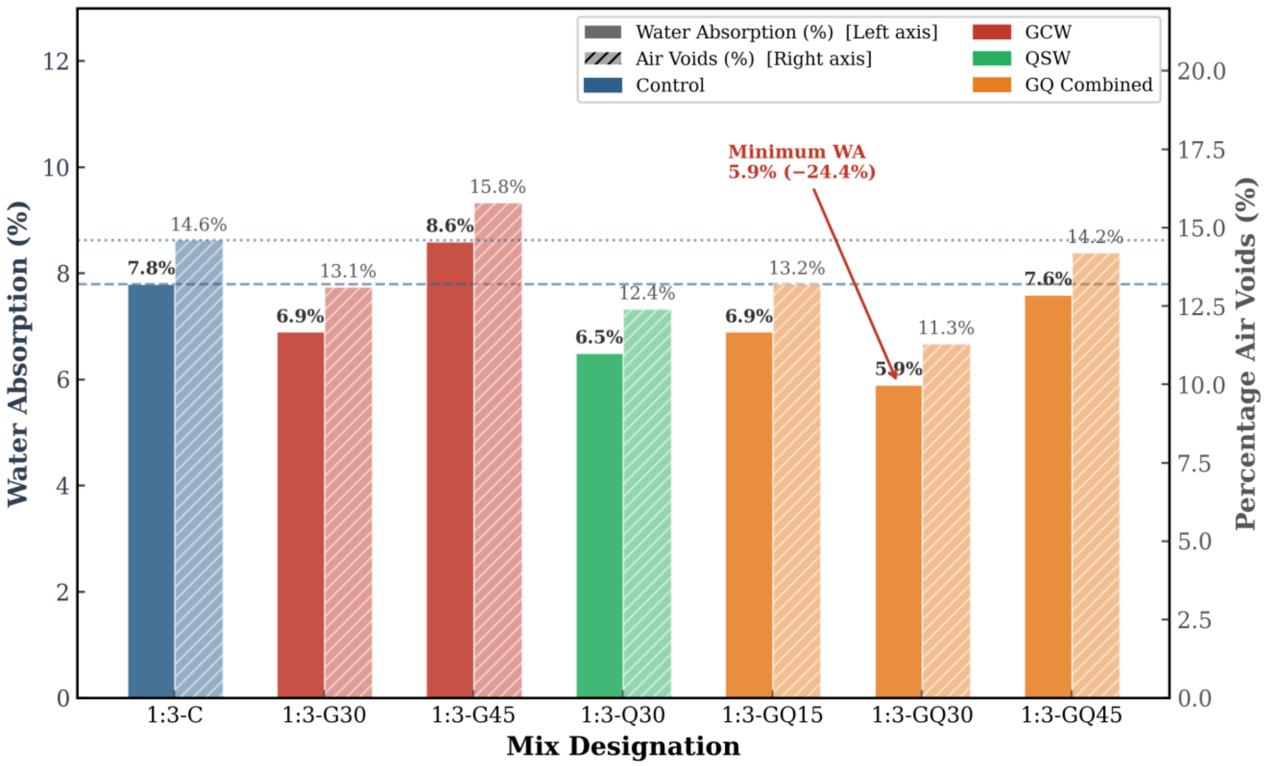

Fig. 3. Water absorption (%) and percentage air voids for selected 1:3 series mixes at 28 days.

4.5 Drying Shrinkage

The drying shrinkage of the 1:3 series mixes, monitored over 90 days, is presented in Fig. 5. The GCW-incorporated mixes exhibited progressive increases in drying shrinkage with increasing replacement level, reaching a maximum final shrinkage of 865×10^{-6} for the G45 mix (a 25.4% increase over the control's 690×10^{-6}), attributable to the elevated water demand and higher evaporable water content associated with the finer GCW particles. Conversely, the QSW-incorporated mixes exhibited a reduction in shrinkage at the 30% level (625×10^{-6}, −9.4% vs control), and the GQ30 mix achieved the lowest overall final shrinkage of 642×10^{-6} (−7.0% vs control), indicating that the combined incorporation of GCW and QSW at the 30% level imparts a marginal but statistically consistent improvement in dimensional stability relative to the conventional mortar. The restraining effect of the angular QSW particles on shrinkage cracking propagation, analogous to the fiber-reinforcing mechanism described by Acar et al. [8] for perlite-based composites, is proposed as the primary physical mechanism underlying this behaviour.

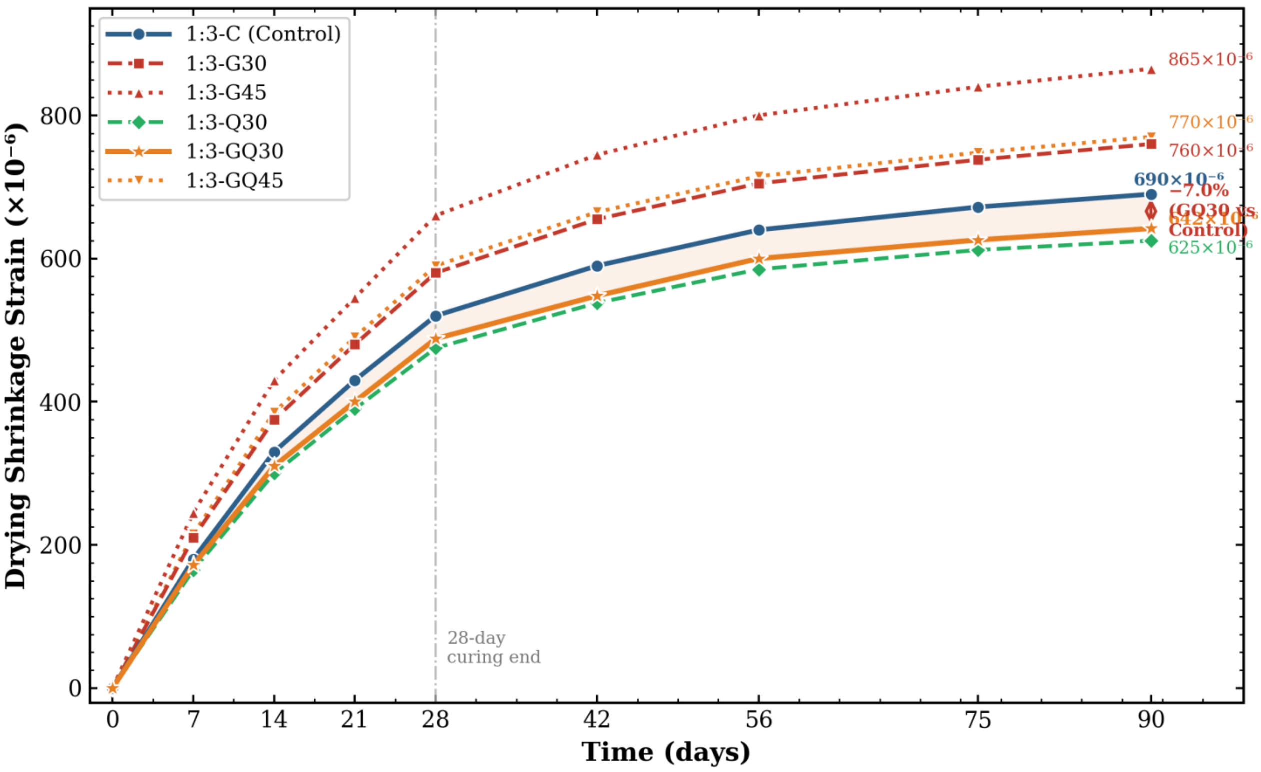

Fig. 4. Drying shrinkage development over 90 days for selected 1:3 series mortar mixes.

4.6 Sulphate Attack Resistance

Table 6 presents the percentage loss in compressive strength for selected 1:3 series mixes after immersion in 5% Na_2SO_4 solution over 180 days.

Table 6. Percentage compressive strength loss due to sulphate attack — 1:3 series.

Mix ID	1 day (%)	28 days (%)	90 days (%)	180 days (%)
1:3-C	0.8	7.9	14.6	21.5
1:3-G30	0.7	6.8	12.7	18.6
1:3-G45	1.1	9.6	17.4	25.8
1:3-Q30	0.5	5.4	10.1	14.9
1:3-GQ30	0.4	4.6	8.6	12.7

The GQ30 mix demonstrated superior sulphate attack resistance, recording a minimum 180-day compressive strength loss of 12.7%, representing a 40.9% reduction in the rate of deterioration relative to the control mix (21.5%). The enhanced sulphate resistance of the GQ30 mix is attributed to its refined pore structure, which limits the ingress of sulphate ions and the subsequent formation of expansive reaction products (gypsum and ettringite) within the pore network — the primary mechanism responsible for strength and mass loss under sulphate attack in cement-based materials. These findings corroborate the general principle, well-established in the literature, that reduced

https://doi.org/10.71058/jodac.v10i06007

porosity confers improved chemical attack resistance, as reported by De Medeiros et al. [30] for marble and granite waste-incorporated cementitious systems and Derrouiche et al. [31] for natural pozzolan-incorporated high-performance concrete.

4.7 Microstructural Analysis

SEM micrographs (Fig. 6) reveal that the hardened GQ30 mix exhibits a markedly denser and more homogeneous microstructure compared to the control, characterized by a reduced population of discrete calcium hydroxide (CH) plates, a lower incidence of capillary microcracks, and intimate embedment of fine GCW particles within the calcium silicate hydrate (C-S-H) gel matrix. The angular QSW particles are observed to form closely interlocked interfaces with the surrounding paste without significant interfacial gaps, consistent with the enhanced mechanical strength and bond properties recorded for GQ30 mixes. MIP analysis (Table 7) quantitatively confirms the pore refinement inferred from the SEM observations, with the GQ30 mix exhibiting the lowest total porosity (13.2%), smallest median pore diameter (31.4 nm), and the highest proportion of gel pores below 50 nm (70.3%) among the mixes examined.

Table 7 Pore structure characteristics from MIP analysis 1:3 series (28 days).

Mix ID	Total Porosity (%)	Median Pore Dia. (nm)	Threshold Pore Dia. (nm)	Pores <50 nm (%)
1:3-C	16.8	42.5	78.6	58.2
1:3-G45	19.6	51.3	92.4	49.6
1:3-Q30	14.9	36.8	68.2	64.7
1:3-GQ30	13.2	31.4	59.5	70.3

The MIP data establish a direct mechanistic link between improved particle packing in the GQ30 formulation and the observed improvements in mechanical and durability performance. The progressive refinement of the pore structure — marked by reduced total porosity, finer median pore diameter, and a higher proportion of fine gel pores relative to coarse capillary pores — reduces the connectivity of the transport network responsible for the ingress of aggressive agents. These microstructural characteristics are consistent with the Gel/Space ratio concept that underpins the strength-porosity relationship in cementitious materials, and corroborate similar findings reported by Arunachalam et al. [15] for copper mine tailing-incorporated cement mortar and by Ainomugisha et al. [11] for sugarcane bagasse ash-blended cement systems.

XRD analysis of the hardened mortar specimens confirmed quartz ($2\theta = 26.65°$) as the dominant crystalline phase in all mixes, with the GQ30 mix exhibiting markedly stronger quartz reflections

https://doi.org/10.71058/jodac.v10i06007

relative to the control, consistent with the elevated quartz content contributed by both GCW and QSW. Crucially, the intensity of the portlandite (calcium hydroxide) peaks at 2θ = 18.0° and 34.1° was observed to be lower in the GQ30 mix compared to the control, suggestive of a minor degree of pozzolanic calcium hydroxide consumption attributable to the finest reactive silicate fraction present within GCW, in addition to the dilution effect arising from partial sand replacement. This XRD observation is consistent with the FTIR spectral evidence of increased C-S-H gel phase intensity (Si-O stretching band, ~960–980 cm^{-1}) in the GQ30 mix, together providing chemical evidence that corroborates the mechanical and microstructural improvements documented in Sections 4.2–4.4. The complementary chemical and physical contributions of GCW (filler + limited pozzolanic action from feldspathic fine fraction) and QSW (inert siliceous filler + mechanical interlock through particle angularity) together constitute a multi-mechanism improvement pathway that neither waste material alone can deliver to the same extent, explaining the consistent superiority of the GQ series over the G and Q single-waste series at equivalent total replacement levels.

4.8 Wetting-Drying Cycle Resistance

Table 8 presents the percentage weight change and visual deterioration assessment for selected 1:3 series mixes after 20 wetting-drying cycles conducted per BS EN 14066:2013.

Table 8. Percentage weight change and visual condition after 20 wetting-drying cycles — 1:3 series.

Mix ID	Weight Change (%)	Visual Condition After 20 Cycles
1:3-C	2.4	Minor surface erosion at corners and edges
1:3-G30	2.1	Negligible surface erosion; intact edges
1:3-G45	3.2	Visible surface erosion; hairline cracks at edges
1:3-Q30	1.8	No visible deterioration; intact surface
1:3-GQ30	1.5	No visible deterioration; intact edges and surface

The wetting-drying cycle results demonstrate that the GQ30 mix exhibited the lowest percentage weight change of 1.5% after 20 cycles — a reduction of 37.5% compared to the control (2.4%) — and showed no visible signs of surface deterioration, cracking, or material loss, while the G45 mix recorded the greatest weight change (3.2%, +33.3% above control) accompanied by visible surface erosion and hairline cracking at specimen edges. The enhanced resistance of the GQ30 mix to cyclic wetting and drying exposure is attributed to the same microstructural densification mechanisms established in the preceding sections: the refined pore structure limits the rate of moisture ingress and egress during each cycle, thereby reducing the internal hygral stresses responsible for surface scaling and microcracking, while the lower drying shrinkage established in Section 4.5 constrains the overall

https://doi.org/10.71058/jodac.v10i06007

volumetric strain amplitude of each cycle. Conversely, the G45 mix, which exhibited the highest drying shrinkage and greatest porosity, experienced the most pronounced hygral strain cycling per cycle, leading to progressive accumulation of microcracking damage and consequently greater material loss. These findings are consistent with the broader literature principle that pore structure refinement confers simultaneous benefits across multiple durability parameters, a relationship corroborated in the context of stone waste utilization by Chouhan et al. [27,28] for limestone waste-incorporated cement mortar and by Adediran et al. [9] for slag-incorporated cement mortar systems.

4.9 Comparative Analysis with Prior Literature

The performance improvements documented for the GQ30 mix in the present study are benchmarked against comparable findings from the recent literature in Table 9, encompassing studies on granite waste, sandstone-derived waste, and combined stone waste utilization in cement-based products. This comparison contextualizes the present findings within the broader framework of stone waste valorization research and highlights both the consistency and the distinctive contributions of the combined GCW-QSW system.

Table 9. Comparative summary of mechanical and durability performance improvements reported in selected prior studies on stone and industrial waste utilization in cement mortar.

Reference	Waste Type	Replacement Level	Max. Compressive Strength Gain	Water Absorption Change	Key Observation
Chajec [21]	Granite powder	10–20%	+6 to +12%	Reduced	Physical filler effect; limited pozzolanic activity
Babu Padavala et al. [17]	Granite quarry dust + fly ash	Ternary blend	+15% (ternary)	Reduced	Synergistic pozzolanic + packing effect
Chouhan et al. [27]	Limestone waste	15–25%	+8 to +14%	Reduced 10–18%	Filler effect; improved gradation
Adediran et al. [9]	Fayalite slag + MSWI ash	30% combined	+10 to +16%	Reduced ~20%	Combined slag-ash packing benefit
Belouadah et al. [20]	Glass + marble powder	10–20% combined	+11 to +18%	Reduced ~15%	Complementary packing; partial pozzolanic
Present study (GQ30)	GCW + QSW combined	30% combined (15+15)	+20.3%	Reduced 24.4%	Synergistic packing + interface enhancement

The comparative analysis presented in Table 9 establishes that the combined GCW-QSW system at 30% total replacement achieves compressive strength gains and water absorption reductions that are at the upper end of those reported for analogous combined stone waste systems in the literature. The +20.3% compressive strength improvement documented for the 1:3-GQ30 mix exceeds the gains

https://doi.org/10.71058/jodac.v10i06007

reported by Chajec [21] for granite powder alone (+6 to +12%), is comparable to the best-performing ternary blends reported by Babu Padavala et al. [17] involving a supplementary cementitious material component, and exceeds the improvements reported by Belouadah et al. [20] for the combined glass powder-marble powder system (+11 to +18%). The 24.4% reduction in water absorption for the GQ30 mix is also among the most substantial reported for stone waste replacement systems in cement mortar in the recent literature. Critically, the GQ30 system achieves these improvements using waste materials that require no calcination, alkali activation, or chemical modification — only collection, drying, and sieving — which enhances the practical and economic viability of this approach relative to more energy-intensive supplementary cementitious material processing routes. The combination of technical superiority, environmental benefit, and processing simplicity positions the GQ30 system as a highly promising formulation for immediate practical application in eco-friendly cement mortar and brick manufacturing, subject to the site-specific verification and scale-up investigations recommended in Section 6.

5. Environmental and Economic Implications

The combined utilization of GCW and QSW at the 30% replacement level in cement mortar delivers multidimensional sustainability benefits that extend beyond technical performance. Each tonne of river sand replaced by GCW or QSW directly reduces the demand for riverbed extraction, thereby mitigating the well-documented ecological consequences of sand mining. Simultaneously, the diversion of GCW and QSW from open disposal sites reduces the land area occupied by stone waste dumps, alleviates soil and groundwater contamination risks, and reduces airborne particulate pollution associated with wind-dispersal of dried stone slurry [1,2,3]. The inherently low embodied energy of both waste materials — which require only collection, drying, and sieving rather than energy-intensive extraction and processing — confers a measurable carbon footprint advantage relative to natural river sand procurement, an advantage that is amplified when transportation distances from stone processing clusters to brick manufacturing units are short, as is typically the case in stone-processing regions such as Rajasthan, India.

From an economic perspective, both GCW and QSW are available at negligible direct material cost to end-users given the disposal burden faced by their generating industries, and their use at the 30% replacement level involves minimal additional processing cost beyond the standard mixing protocol. The enhanced mechanical and durability performance of the GQ30 mix further translates to a potential for extended service life of mortar and brick products manufactured with this formulation, reducing lifecycle maintenance and replacement costs for masonry structures. These considerations

https://doi.org/10.71058/jodac.v10i06007

collectively position the GQ30 system as both an environmentally responsible and economically viable alternative to conventional natural sand mortar, consistent with the principles of circular economy design increasingly advocated in the construction materials literature [23,24,25] and aligned with national policy frameworks promoting the valorization of industrial waste in the construction sector [33,34].

6. Conclusions

The present investigation systematically examined the mechanical, durability, and microstructural performance of cement mortar incorporating Granite Cutting Waste (GCW) and Quartz Sandstone Waste (QSW), individually and in equal-proportion combination, as partial substitutes for river sand at 0%, 15%, 30%, and 45% replacement levels at two cement-to-sand ratios (1:3 and 1:6). The following principal conclusions are drawn from the results:

1. A 30% combined replacement of river sand by equal proportions of GCW and QSW (GQ30 mix) achieved the optimal balance of workability, mechanical performance, and durability, yielding a 20.3% improvement in 28-day compressive strength, an 18.1% improvement in flexural strength, and the highest UPV of 3895 m/s and dynamic modulus of 32.3 GPa among all 1:3 series mixes investigated.
2. Water absorption and percentage air voids were minimized in the GQ30 mix (5.9% and 11.3% respectively), representing reductions of 24.4% and 22.6% relative to the control, directly attributable to improved particle packing arising from the complementary particle size distributions of GCW (finer) and QSW (coarser).
3. Drying shrinkage of the GQ30 mix (642×10^{-6} at 90 days) was 7.0% lower than the control, while the G45 mix exhibited a 25.4% increase, confirming that high GCW replacement levels impair dimensional stability due to elevated water demand.
4. The GQ30 mix demonstrated a 40.9% reduction in 180-day compressive strength loss under sulphate attack exposure relative to the control, attributable to its refined and less permeable pore structure.
5. MIP analysis confirmed that the GQ30 mix possessed the lowest total porosity (13.2%), finest median pore diameter (31.4 nm), and highest proportion of fine gel pores (70.3%), providing direct microstructural evidence of the densification mechanism underpinning all observed performance improvements.

https://doi.org/10.71058/jodac.v10i06007

6. A replacement level beyond 45% using GCW alone consistently degraded all performance parameters across both mix ratios investigated, establishing 45% GCW as an upper bound beyond which the dilution effect and increased water demand outweigh the packing benefit.
7. The GQ30 system represents a technically, environmentally, and economically viable formulation for the development of eco-friendly cement mortar and bricks, contributing to resource conservation, reduction of stone waste disposal, and promotion of circular economy principles in the construction sector.

Declaration of Competing Interest

The authors declare that they have no known competing financial interests or personal relationships that could have appeared to influence the work reported in this paper.

Acknowledgements

The authors express their gratitude to [Name of University/Institute] for providing laboratory facilities and to the granite and quartz sandstone processing industries in [Region] for supplying the waste materials used in this study.

Data Availability Statement

The data that support the findings of this study are available from the corresponding author upon reasonable request.

References

[1] Serour A, Khedr MH, Shehata N, Mohamed OA. Designing low-clinker green cement with high bypass dust content: A resource-efficient approach using industrial wastes. Ain Shams Eng J. 2026;17(4):104071. https://doi.org/10.1016/j.asej.2026.104071

[2] Abbas MM. Recycling waste materials in construction: Mechanical properties and predictive modeling of Waste-Derived cement substitutes. Waste Manag Bull. 2025;3(1):168–192. https://doi.org/10.1016/j.wmb.2025.01.004

[3] Abbass M, Akhai S. Eco-friendly geopolymer bricks synthesized from alkali-activated sugarcane bagasse ash and rice husk ash. Ind Crops Prod. 2025;233:121410. https://doi.org/10.1016/j.indcrop.2025.121410

[4] Abbass W, Mahmood SU, Ahmed A, Aslam F, Mohamed A. Comparative analysis of enriched flyash based cement-sand compressed bricks under various curing regimes. Heliyon. 2024;10(5):e26945. https://doi.org/10.1016/j.heliyon.2024.e26945

[5] Abbass W, Mahmood SU, Ahmed A, Aslam F, Mohamed A. Comparative analysis of enriched flyash based cement-sand compressed bricks under various curing regimes. Heliyon. 2024;10(5):e26945. https://doi.org/10.1016/j.heliyon.2024.e26945

[6] Abdalla JA, Hawileh RA, Bahurudeen A, Jyothsna G, Sofi A, Shanmugam V, Thomas BS. A comprehensive review on the use of natural fibers in cement/geopolymer concrete: A step towards sustainability. Case Stud Constr Mater. 2023;19:e02244. https://doi.org/10.1016/j.cscm.2023.e02244

[7] Abdalla JA, et al. A comprehensive review on the use of natural fibers in cement/geopolymer concrete: A step towards sustainability. Case Stud Constr Mater. 2023;19:e02244. https://doi.org/10.1016/j.cscm.2023.e02244

https://doi.org/10.71058/jodac.v10i06007

[8] Acar MC, Çelik Aİ, Kayabaşı R, Şener A, Özdöner N, Özkılıç YO. Production of perlite-based-aerated geopolymer using hydrogen peroxide as eco-friendly material for energy-efficient buildings. J Mater Res Technol. 2023;24:81–99. https://doi.org/10.1016/j.jmrt.2023.02.179

[9] Adediran A, Asaam N, Manso-Morato J, Avci E, Perumal P. Fayalite slag and municipal solid waste incineration bottom ash as sand replacement in cement mortar: Physical, mechanical, and durability properties. J Build Eng. 2026;127:116374. https://doi.org/10.1016/j.jobe.2026.116374

[10] Ahmad F, Rawat S, Yang R(C), Zhang L, Zhang YX. Fire resistance and thermal performance of hybrid fibre-reinforced magnesium oxychloride cement-based composites. Constr Build Mater. 2025;472:140867. https://doi.org/10.1016/j.conbuildmat.2025.140867

[11] Ainomugisha S, Kibwami N, Racheal W, Adubango EN, Matovu MJ, Manga M. Effect of sugarcane bagasse ash on eco-friendly blended cement production: Physicochemical, mechanical, and microstructure properties. Case Stud Constr Mater. 2025;22:e04141. https://doi.org/10.1016/j.cscm.2024.e04141

[12] Akinwande AA, Oyediran AO, Balogun OA, Balogun RB, El Hachem C, Accouche O, Azab M. Experimental analysis and optimization of kenaf fiber-lateritic bricks using glass powder as partial cement replacement. Sci Afr. 2024;26:e02457. https://doi.org/10.1016/j.sciaf.2024.e02457

[13] Al-Fakih A, Abujamil A, Al-Shugaa MA, Assaggaf R, Al-Osta MA, Shaqraa AA. Utilization of ceramic polishing sludge in masonry cement mortar: Mechanical strength and thermal behavior. Results Eng. 2025;27:107058. https://doi.org/10.1016/j.rineng.2025.107058

[14] Arumugam H, Iqbal MM, Ahn C-H, Rimdusit S, Muthukaruppan A. Development of high performance granite fine fly dust particle reinforced epoxy composites. J Mater Res Technol. 2023;24:2795–2811. https://doi.org/10.1016/j.jmrt.2023.03.199

[15] Arunachalam KP, Avudaiappan S, Maureira N, Da Costa Garcia Filho F, Monteiro SN, Batista ID, De Azevedo ARG. Innovative use of copper mine tailing as an additive in cement mortar. J Mater Res Technol. 2023;25:2261–2274. https://doi.org/10.1016/j.jmrt.2023.06.066

[16] Atasham Ul Haq M, Wang P, Gong F, Hassam M, Iqbal MS, Li W, Tahir M. Influence of agricultural waste ash slurry-treated recycled brick aggregates on the mechanical and durability performance of concrete. Case Stud Constr Mater. 2026;24:e05794. https://doi.org/10.1016/j.cscm.2026.e05794

[17] Babu Padavala SSA, Dey S, Veerendra GTN, Manoj AVP. Performance evaluation of ternary blended cement concrete partially replacement of natural sand with granite quarry dust. Hybrid Adv. 2023;4:100082. https://doi.org/10.1016/j.hybadv.2023.100082

[18] Bahmani H, Mostofinejad D, Eftekhar MR. A novel eco-friendly thermal-insulating high-performance geopolymer concrete containing calcium oxide-activated materials. Dev Built Environ. 2024;18:100473. https://doi.org/10.1016/j.dibe.2024.100473

[19] Bahmani H, Mostofinejad D, Eftekhar MR. A novel eco-friendly thermal-insulating high-performance geopolymer concrete. Dev Built Environ. 2024;18:100473. https://doi.org/10.1016/j.dibe.2024.100473

[20] Belouadah M, Rahmouni ZEA, Tebbal N. Influence of the addition of glass powder and marble powder on the physical and mechanical behavior of composite cement. Procedia Comput Sci. 2019;158:366–375. https://doi.org/10.1016/j.procs.2019.09.064

[21] Chajec A. The use of granite powder waste in cementitious composites. J Mater Res Technol. 2023;25:4761–4783. https://doi.org/10.1016/j.jmrt.2023.06.253

[22] Chajec A, Šavija B. The effect of using surface functionalized granite powder waste on fresh properties of 3D-printed cementitious composites. J Build Eng. 2024;97:110707. https://doi.org/10.1016/j.jobe.2024.110707

[23] Char M, Tilioua A. Recycling of geosourced materials through geopolymerization: Towards sustainable and high-performance earth bricks for resilient construction. Next Mater. 2025;9:101293. https://doi.org/10.1016/j.nxmate.2025.101293

[24] Chen L, Zhao X, Liu J, Ma H, Wang C, Zhang H, Wang J. Progress on rock mechanics research of Beishan granite for geological disposal of high-level radioactive waste in China. Rock Mech Bull. 2023;2(3):100046. https://doi.org/10.1016/j.rockmb.2023.100046

[25] Chougan M, et al. Comparative analysis of ternary blended cement with clay and engineering brick aggregate for high-performance 3D printing. Dev Built Environ. 2024;20:100529. https://doi.org/10.1016/j.dibe.2024.100529

[26] Chougan M, et al. Comparative analysis of ternary blended cement with clay and engineering brick aggregate for high-performance 3D printing. Dev Built Environ. 2024;20:100529. https://doi.org/10.1016/j.dibe.2024.100529

https://doi.org/10.71058/jodac.v10i06007

[27] Chouhan HS, Kalla P, Nagar R, Gautam PK. Gainful utilization of dimensional limestone waste as fine aggregate in cement mortar mixes. Constr Build Mater. 2019;221:363–374. https://doi.org/10.1016/j.conbuildmat.2019.06.097

[28] Chouhan HS, Kalla P, Nagar R, Gautam PK. Gainful utilization of dimensional limestone waste as fine aggregate in cement mortar mixes. Constr Build Mater. 2019;221:363–374. https://doi.org/10.1016/j.conbuildmat.2019.06.097

[29] Da Silva JB, Zat T, Werner ES, Brehm FA, Gonçalves JP, Souza MT, Rodríguez ED. Recycling of municipal sewage sludge for the manufacture of environmentally friendly ceramic bricks. Case Stud Constr Mater. 2024;21:e03610. https://doi.org/10.1016/j.cscm.2024.e03610

[30] De Medeiros WRP, De Medeiros Melo Neto O, Luz PMSG, Oliveira RKFD, Guedes LR. Utilizing marble and granite industry waste in asphalt mixtures for enhanced road performance and sustainability. J Eng Res. 2024;12(4):670–679. https://doi.org/10.1016/j.jer.2023.10.032

[31] Derrouiche Y, Achoura D, Saliba J, Cassagnabère F. Natural pozzolan as a sustainable cement replacement in high-performance concrete: Effects on mechanical properties, durability, and microstructural development. Sci Afr. 2025;27:e02574. https://doi.org/10.1016/j.sciaf.2025.e02574

[32] Diao Y, Zhu D, Hu Q, Zhang L, Wang C, Huang J. Stabilization strategies for granite waste powder applied in sustainable pavement subgrade: Mechanical and durability performance. Case Stud Constr Mater. 2024;21:e03802. https://doi.org/10.1016/j.cscm.2024.e03802

[33] Douidi O, Tafraoui A, Serna P, Makani A, Ferrara L. Exploring the feasibility of using recycled fines from diverse sources as partial cement substitutes in high-performance cementitious materials. Results Eng. 2026;29:108506. https://doi.org/10.1016/j.rineng.2025.108506

[34] El Fadili H, Ben Ali M, Moussadik A, El Mahi M, Rahman MN, Lotfi EM. Synthesis of eco-friendly alkali-activated materials based on incineration by-products and cigarette filters. Cleaner Eng Technol. 2024;23:100849. https://doi.org/10.1016/j.clet.2024.100849

[35] El-Sayed HA, Farag AB, Kandeel AM, Younes AA, Yousef MM. Characteristics of the marble processing powder waste and its suitability for cement manufacture. HBRC J. 2018;14(2):171–179. https://doi.org/10.1016/j.hbrcj.2016.06.002

[36] El-Sayed HA, Farag AB, Kandeel AM, Younes AA, Yousef MM. Characteristics of the marble processing powder waste and its suitability for cement manufacture. HBRC J. 2018;14(2):171–179. https://doi.org/10.1016/j.hbrcj.2016.06.002

[37] El-Yahyaoui A, Manssouri I. Clay and smmar plant fibers: A sustainable approach to unfired bricks for eco-friendly construction. Next Mater. 2026;12:102255. https://doi.org/10.1016/j.nxmate.2026.102255

[38] El-Yahyaoui A, Manssouri I. Clay and smmar plant fibers: A sustainable approach to unfired bricks for eco-friendly construction. Next Mater. 2026;12:102255. https://doi.org/10.1016/j.nxmate.2026.102255

[39] Farooq U, Rizwan M, Khaliq W, Ejaz A, Saingam P, Hussain Q, Joyklad P. Towards sustainable construction: Harnessing potential of pumice powder for eco-friendly concrete, augmented by hybrid fiber integration. Case Stud Constr Mater. 2024;21:e03815. https://doi.org/10.1016/j.cscm.2024.e03815

[40] Fellah M, Ouhaibi S, Belouaggadia N, Mansouri K, Sebaibi N. Enhancing building energy efficiency across diverse climatic zones in Morocco through optimized eco-friendly insulation thickness with air gap. Energy Rep. 2024;12:1551–1565. https://doi.org/10.1016/j.egyr.2024.07.040